JOURNAL OF AGRICULTURAL AND FOOD CHEMISTRY

pubs.acs.org/JAFC Article

Antifungal Mechanism of Volatile Organic Compounds Produced by *Bacillus subtilis* CF-3 on *Colletotrichum gloeosporioides* Assessed Using Omics Technology

Ke Wang,[†] Zhen Qin,[†] Shiyuan Wu, Pengyu Zhao, Chaoying Zhen, and Haiyan Gao*

Cite This: *J. Agric. Food Chem.* 2021, 69, 5267−5278 Read Online

ACCESS | Metrics & More | Article Recommendations | Supporting Information

ABSTRACT: *Bacillus subtilis* is commonly used as a biocontrol bacterium owing to its strong antifungal activity, broad-spectrum inhibition, and general safety. In this study, the inhibitory effects of volatile organic compounds (VOCs) produced by *B. subtilis* CF-3 on *Colletotrichum gloeosporioides*, a major destructive phytopathogen of litchi anthracnose, were analyzed using proteomics and transcriptomics. Differentially expressed genes (DEGs) and proteins (DEPs) indicated that the inhibition of *C. gloeosporioides* by *B. subtilis* CF-3 VOCs downregulated the expression of genes related to cell membrane fluidity, cell wall integrity, energy metabolism, and production of cell wall-degrading enzymes. Particularly, those important DEGs and DEPs related to the ergosterol biosynthetic and biosynthesis of unsaturated fatty acids are most significantly influenced. 2,4-di-*tert*-butylphenol, a characteristic component of *B. subtilis* CF-3 VOCs, also showed a similar effect on *C. gloeosporioides*. Our results provide a theoretical basis for the potential application of *B. subtilis* CF-3 in the postharvest protection of fruits and vegetables.

KEYWORDS: *Bacillus subtilis, volatile organic compounds, anthracnose, transcriptomics, proteomics*

Downloaded via haiyan gao on May 9, 2021 at 00:35:02 (UTC).
See https://pubs.acs.org/sharingguidelines for options on how to legitimately share published articles.

INTRODUCTION

Postharvest diseases are one of the main causes of postharvest loss of fruit and vegetable crops. The most prominent plant pathogenic fungi that cause postharvest rot include *Botrytis* spp.,[1] *Penicillium* spp.,[2] *Aspergillus* spp.,[2] *Alternaria* spp.,[3] *Fusarium* spp.,[4] *Colletotrichum* spp.,[4] and *Monilinia* spp.[4] Among them, *Colletotrichum* spp. is a considerably pathogenic fungus that infects fruits. Owing to its wide host range and rapid growth, *Colletotrichum* spp. causes anthracnose spot and rot symptoms in fruits, which results in significant economic losses.[5,6] Currently, anthracnose is predominantly treated or prevented using chemical fungicides such as copper oxychloride, cupric hydroxide, benomyl, methyl thiophanate, carbendazim, thiabendazole, and difenoconazole.[7] Although chemical pesticides have played an important role in the control of plant diseases, their use is associated with risks, including the accumulation of toxic compounds that are potentially dangerous to humans and the environment, which has become a major concern. Furthermore, an increasing number of pathogen strains shows resistance to fungicides.[8]

As an alternative to chemical fungicides for counteracting anthracnose, antagonistic microorganisms may be used for culture control.[9] Several species of the genus *Bacillus* have been reported to inhibit the growth of several plant pathogens and have been used increasingly as biological control agents against plant pathogens.[10] Previous studies indicated that *Bacillus subtilis* are known for their ecofriendly nature, generally recognized as safe, and show a broad inhibitory spectrum against postharvest pathogens of fruits.[11] Moreover, recent studies reported that *B. subtilis* can produce not only antibiotics and antifungal proteins[12] but also a series of volatile organic compounds (VOCs),[13] which can effectively inhibit the growth of postharvest pathogens of fruits and vegetables. In our previous study, the *B. subtilis* strain CF-3, which is used as a biocontrol agent, was isolated and identified.[14] VOCs from the *B. subtilis* CF-3 fermentation broth show considerable antifungal effects.[15,16] The compounds possibly generated by CF-3 are listed in the Table S1. Furthermore, 2,4-di-*tert*-butylphenol (DTBP) was found to be a vital VOC component of the *B. subtilis* CF-3 fermentation broth, which showed strong inhibitory effects on the plant pathogenic fungus *Colletotrichum gloeosporioides*.[17] Compared with the nonvolatile antifungal substances, VOCs are more likely to exert antifungal activity via air and soil. Moreover, VOCs do not easily produce drug resistance and do not damage the environment.[18] Looking forward to the application prospect of VOCs, it can be combined with the modified atmosphere storage in order to achieve anticorrosion. However, the present research on VOCs of their antifungal mechanism is relatively rare. Most of the VOC research reports focused on the action of their nutritional spatial competition as well as in vitro inhibition of spore germination. The study on the prevention and control of biocontrol mechanisms of postharvest diseases of fruits and vegetables is not yet thorough. The clear antifungal mechanism will be more conducive to the precise development of efficient biocontrol

Received: February 1, 2021
Revised: April 13, 2021
Accepted: April 13, 2021
Published: April 26, 2021

© 2021 American Chemical Society

https://doi.org/10.1021/acs.jafc.1c00640
J. Agric. Food Chem. 2021, 69, 5267−5278

agents. In particular, there are few research studies that focus on its molecular mechanism. This will slow down the research and development of its biological control agents.

With the next-generation sequencing (NGS) technology, RNA sequencing has been used extensively in the understanding of biological and physiological processes of many fungal species.[19,20] Tandem mass tag (TMT)-based quantitative proteomics has been widely used and has been proven to be a reliable method for determining protein expression levels.[21,22] As gene expression is also regulated by post-transcriptional modification and translation processes, additional proteomic analysis is also imperative for a complete comprehension of the molecular mechanisms.[23] Proteomics and transcriptomics are increasingly used in the study of postharvest fruit diseases, which are also essential for the complete understanding of the molecular mechanisms of postharvest disease control.[24−26]

In this study, we assessed the antifungal mechanism of fermentation broth VOCs of *B. subtilis* CF-3 and its characteristic component DTBP on *C. gloeosporioides* using transcriptomics and proteomics. Our results revealed that the mechanisms of VOCs produced by *B. subtilis* CF-3 affect transcriptional regulation, protein expression, and metabolic pathways of *C. gloeosporioides*, which provides a theoretical basis for the development of biological control agents.

MATERIALS AND METHODS

Strain. *B. subtilis* CF-3 (registered in the China Center for Type Culture Collection; CCTCC M 2016125) was isolated from fermented bean curd and was identified at the Laboratory of Food Safety and Quality Control.[27] To produce fermentation broth, *B. subtilis* CF-3 was cultivated on Luria-Bertani (LB) solid medium at 37 °C for 24 h, gently scraped off using an inoculation loop, transferred to 100 mL of LB liquid medium in a conical flask, and cultivated at 37 °C in a rotary shaker at 150 rpm for 24 h. The concentration of the solution was adjusted to 10^8 colony-forming units (CFU)/mL, after which it was stored until use.

C. gloeosporioides was obtained from the Institute of Environment and Plant Protection, Chinese Academy of Tropical Agricultural Sciences (registered in Agricultural Culture Collection of China; ACCC 36351) and was cultured at 28 °C on potato dextrose agar medium (PDA) before use in experiments.

The method about the plate enthalpy test described by Arrebola et al.[27] and Jiang et al.[28] was used to assess the inhibitory effects of VOCs produced by *B. subtilis* CF-3 on *C. gloeosporioides*. Briefly, 20 μL of 10^8 CFU/mL *B. subtilis* CF-3 fermentation broth (VOC group) and 1 mol/L DTBP (DTBP group) were evenly spread on solid LB medium. Distilled water (20 μL) was used as control. Subsequently, we punched out a culture plug (7 mm diameter) from the agar of the fungal cultures that were incubated for 7 days, and then, we placed the culture plug at the center of a PDA medium plate. Then, the LB solid medium was inverted and placed on the fungus-attached PDA solid medium, and Petri dishes were sealed using parafilm to reduce the loss of VOCs. The cultures were incubated in an electrothermal incubator at 28 °C for 7 days, after which the pathogenic fungal mycelium was harvested and stored at −80 °C until RNA isolation. Each treatment was performed in triplicate.

RNA Isolation and Sequencing Library Preparation. Total RNA of mycelia was extracted from the control group, VOC treatment group, and DTBP treatment group. RNA isolation was performed using Trizol reagent (Invitrogen, New Jersey, USA) following the manufacturer's instructions. RNA concentrations were measured using a NanoDrop 2000 spectrophotometer (Thermo Fisher Scientific, Waltham, USA). RNA integrity was assessed using the RNA Nano 6000 Assay Kit of the Agilent Bioanalyzer 2100 system (Agilent Technologies, Santa Clara, CA, USA). One microgram RNA per sample was used as input for sequencing library preparation. cDNA libraries were produced using an NEB Next Ultra RNA Library Prep Kit (New England Biolabs, Inc., Ipswich, USA) for Illumina following the manufacturer's instructions. PCR products were purified (Agencourt AMPure XP System; Beckman Coulter, Brea, CA, USA), and library quality was assessed using an Agilent Bioanalyzer 2100 system (Agilent Technologies, Santa Clara, CA, USA). Finally, the cDNA libraries were sequenced on a flow cell using an Illumina HiSeq 2500 sequencing platform (Biomarker Tech, Beijing, China). For each treatment, three samples were prepared in parallel for transcriptomics analysis.

Transcriptomics Bioinformatic Analysis. Raw data were quality-filtered [Q values (≤30) higher than 30%] to retain only clean reads. The fragments per kilobase of transcript per million fragments mapped (termed FPKM[29]) were used to calculate gene expression levels. Before analysis of differential gene expression, read counts of each library were adjusted using a scaling normalization factor with the edgeR package, and differential expression analysis of two samples was performed using the EBSeq R package.[30] Regarding differentially expressed genes (DEGs), differential expression was determined as DEGs with fold change ≥ 2 and FDR < 0.01 as screening criteria.

An in-depth analysis based on DEGs was performed, including comparison using the Blast2GO program and the NCBI non-redundant protein database (http://www.geneontology.org), implemented by the Kolmogorov−Smirnov test based on the topGO R package Enrichment analysis of gene ontology (GO) of DEGs, using KOBAS[31] software to statistically test the enrichment of DEGs in the Kyoto Encyclopedia of Genes and Genomes (KEGG) pathway.

Validation of RNA Sequencing. To validate the results of RNA sequencing, 12 DEGs (six downregulated and six upregulated DEGs from each of the two treatments) were selected for real-time reverse transcription PCR (RT-PCR). Total RNA was extracted from each sample using Trizol reagent (Invitrogen). RNA was quantified using a NanoDrop2000 spectrophotometer (Thermo Fisher Scientific, Waltham, USA), and integrity was assessed by agarose gel electrophoresis. cDNA was synthesized using MasterMix (TaKaRa, Dalian, China). RT-PCR was performed using a TB Green qPCR Kit (TaKaRa, Dalian, China) with the following thermocycling conditions: 95 °C for 30 s, followed by 40 cycles of 95 °C for 5 s and 60 °C for 30 s. After the reaction was completed, the amplification curve and melting curve of the RT-PCR were constructed, and the data were analyzed. All samples were tested in triplicate. The target genes and the respective PCR primers are shown in Table S2.

Protein Extraction, Quantification, and Liquid Chromatography with Tandem Mass Spectrometry Analysis. A protein extraction kit (MYP1900, MesGenBiotech, Tianjin, China) was used to extract the total protein from the samples. A BCA Protein Assay kit (Beyotime Biotechnology, Shanghai, China) was used to determine protein concentrations, and SDS-PAGE was performed to verify protein quality. Protein digestion, peptide desalting, and TMT peptide labeling were carried out using samples that met the quality requirements.

Reconstituted peptide solutions were used for liquid chromatography with tandem mass spectrometry (LC−MS/MS) analysis, and each sample fraction was injected once for a total of 15 mass spectrometric analysis. An appropriate amount of peptide was taken from each sample and was chromatographically separated using the nanoflow liquid chromatography system EASY-nLC 1200 (Thermo Fisher Scientific, Waltham, USA). The mobile phase was a mixture of water containing 0.1% formic acid and acetonitrile with 0.1% formic acid, isocratically delivered by a pump at a flow rate of 300 nL/min. The elution gradient was as follows: 0−2 min, 4−7% B; 2−67 min, 7−20% B; 67−79 min, 20−35% B; 79−81 min, 30−90% B; 81−90 min, 90% B. After peptide separation, a Q-Exactive Plus mass spectrometer (Thermo Fisher Scientific, Waltham, USA) was used for data-dependent acquisition mass spectrometry. The following settings were used: analysis time: 90 min, detection method: positive ion, and precursor ion scanning range: 300−1800 m/z. The mass-to-charge ratio of peptides and fragments of peptides was collected according to

https://doi.org/10.1021/acs.jafc.1c00640
J. Agric. Food Chem. 2021, 69, 5267−5278

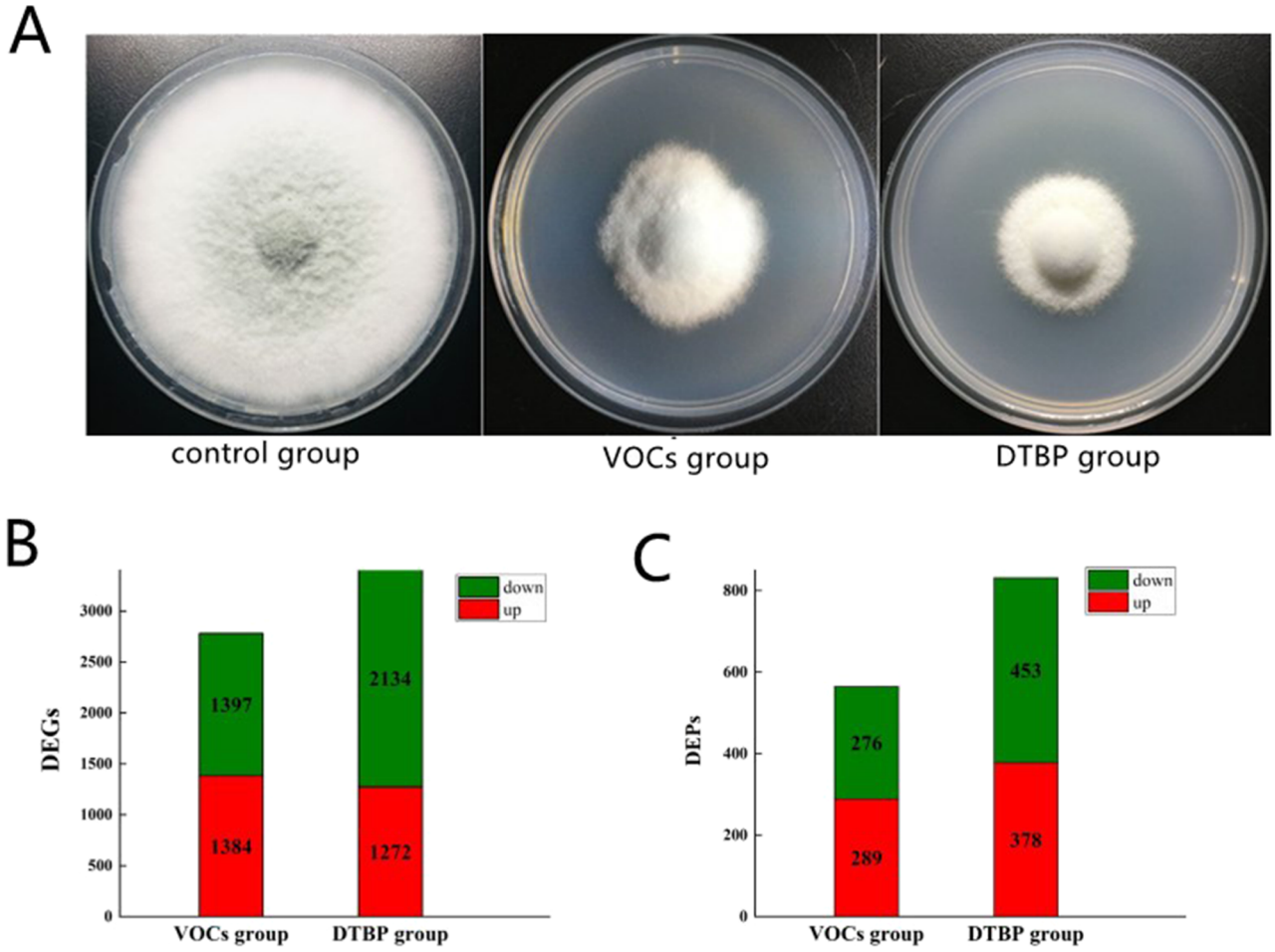

Figure 1. Effect of treatment groups on *C. gloeosporioides* growth, genes, and proteins. (A) *B. subtilis* CF-3 inhibited the growth and germination of *C. gloeosporioides*. *C. gloeosporioides* in the plates, treated with distilled water, *B. subtilis* CF-3 fermentation broth VOCs, and DTBP. (B) Numbers of DEGs in both treatment groups. (C) Numbers of DEPs in both treatment groups.

the following method: 20 fragment maps were collected after each full scan. The following settings were used: first-level mass spectrometry resolution: 70,000 at m/z 200, AGC target: 1×10^6, first-level maximum IT: 50 ms; secondary mass spectrometry resolution: 35,000 at m/z 200, AGC target: 1×10^5, secondary maximum IT: 50 ms, MS2 activation type: HCD, isolation window: 1.6 Th, normalized collision energy: 35.

Proteomics Bioinformatic Analysis. The original LC−MS/MS raw files were imported into the search engine Sequest HT in Proteome Discoverer software (version 2.2) for database retrieval. The database used for the database search was Uniprot. *C. gloeosporioides*_GC5_15380_201181122.fasta, which was obtained from the protein database on the website https://www.uniprot.org/uniprot/?query=taxonomy:474922, and 15,380 proteins were used.

The functional annotation of *C. gloeosporioides* protein database is limited; therefore, we selected multiple related species for protein database comparison (using BLAST). Based on the results of the database search and functional protein comparison, we used the corresponding GENE ID/Symbol obtained by the comparison for the subsequent bioinformatic analysis.

The threshold for differential protein expression was a fold change of >1.2 or <0.83 and $P < 0.05$ in the respective statistical test. Annotations of biological functions of proteins mainly involve protein ontology (GO) annotation[32] and KEGG biological pathway analysis[33] (termed KEGG pathway). GO annotation was performed using Blast2GO software for comparison within the nonredundant NCBI protein database (http://www.geneontology.org). Biological pathway classification and grouping of identified proteins were performed using the KEGG database (http://www.genome.jp/kegg/). Annotation of biological functions of proteins is predominantly based on the extraction of information from GO and KEGG. Statistical analysis of GO and KEGG enrichment data was carried out using Fisher's exact test, and FDR correction for multiple testing was performed.

RESULTS

Effects of *B. subtilis* CF-3 VOCs on *C. gloeosporioides* Growth. To explore the *in vitro* biocontrol effects of fermentation broth VOCs of *B. subtilis* CF-3 on fungal pathogens, colony sizes, and morphology of *C. gloeosporioides* were documented 7 days after inoculation. As shown in Figure 1A, the circular diameters of *C. gloeosporioides* colonies were only 30 and 26 mm, respectively, after treatment with *B. subtilis* CF-3 VOCs and DTBP. *C. gloeosporioides* mycelium of the control treatment covered almost the entire plate (68 mm) after 7 days of cultivation, whereas in both treatments, *C. gloeosporioides* growth was strongly inhibited. Mycelia from these cultures were further examined using omics techniques.

Overview of Transcriptome and RT-PCR Validation. High-throughput RNA sequencing produced 111.22 Gb of clean sequence data. The GC content of all samples exceeded 53%. The Q30 base percentage was at least 92.86%. Bulk sequencing statistics are summarized in Table S3. The sequencing data were of adequate quality and were considered suitable for further analysis. To validate gene expression data obtained from RNA sequencing, we selected 12 DEGs (6

https://doi.org/10.1021/acs.jafc.1c00640
J. Agric. Food Chem. 2021, 69, 5267−5278

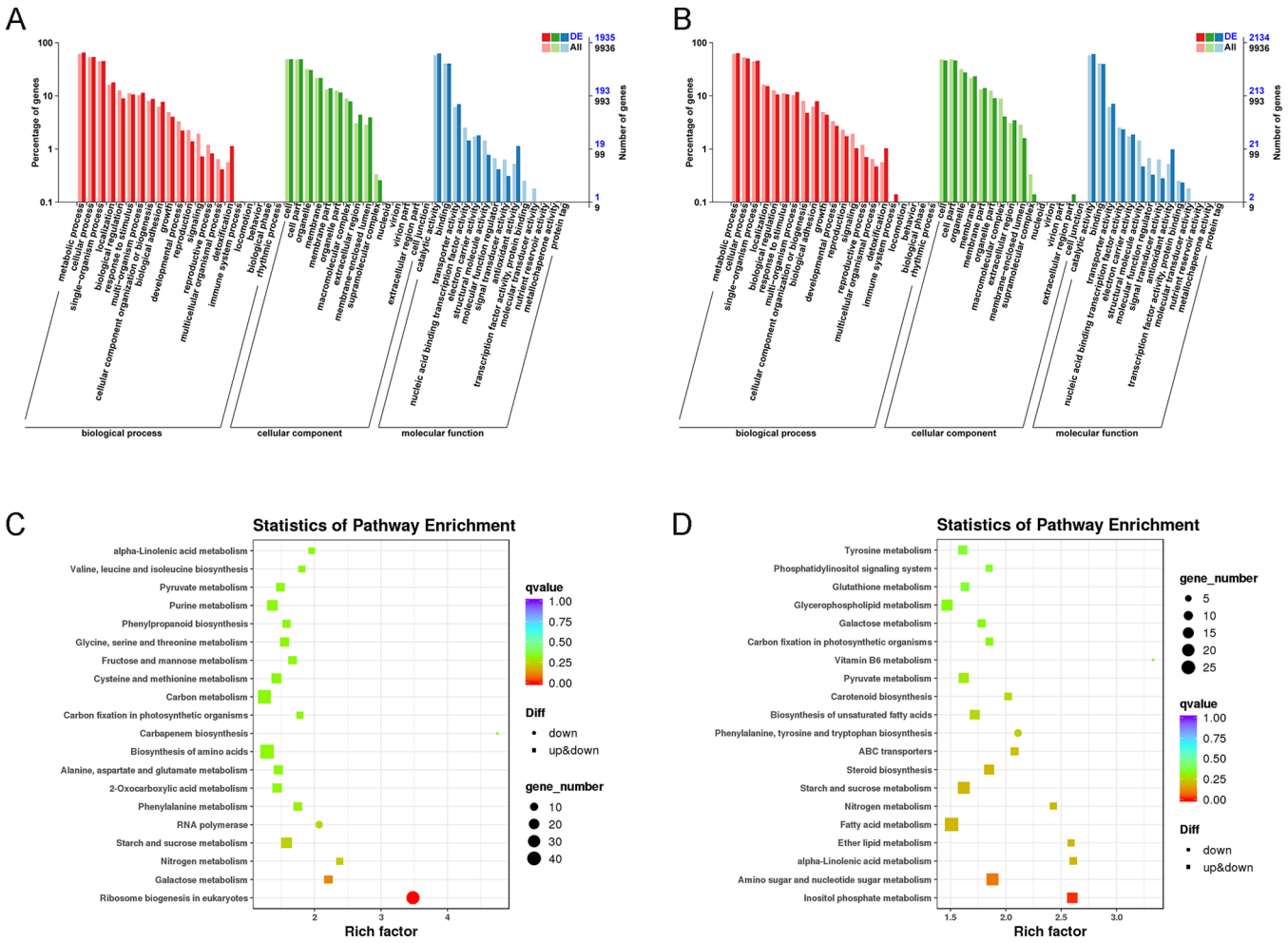

Figure 2. Functional annotation of DEGs. (A) Gene Ontology (GO) enrichment analysis for DEGs of the VOCs group. (B) GO enrichment analysis for DEGs of the DTBP group. (C) KEGG pathway enrichment scatter plot of DEGs in the VOCs group. (D) KEGG pathway enrichment scatter plot of DEGs in the DTBP group. Treatments are represented using different colors.

downregulated and 6 upregulated DEGs) to quantify expression levels using RT-PCR. RNA sequencing and RT-PCR analysis showed consistent expression trends for each of the analyzed candidate genes (Figure S1), suggesting that the transcriptomic data were adequate for further functional analysis and mechanistic interpretation.

DEGs were identified by comparing RNA sequence data from the VOCs and DTBP treatment with that of the control group. In total, 2781 DEGs (1384 upregulated and 1397 downregulated genes) were observed in the VOC treatment and 3406 DEGs (1272 upregulated and 2134 downregulated DEGs) in the DTBP treatment (Figure 1B). Comparing the two groups of DEGs, there were 1229 DEGs in total, of which 1090 showed the same trend and 139 produced opposite trends.

Functional Annotation of DEGs. Based on GO functional analysis, the identified DEGs were classified into three major categories: molecular functions, cellular components, and biological processes (Figure 2A,B). In the VOC treatment (Figure 2A), 1935 DEGs (999 upregulated and 936 downregulated DEGs) were identified using GO functional analysis. In the category of molecular functions, "catalytic activity" (673 upregulated and 535 downregulated DEGs) was the most frequent term, followed by "transporter activity" (64 upregulated and 71 downregulated DEGs) and "binding" (364 upregulated and 420 downregulated DEGs). In the category of cellular components, the most highly enriched terms were "cell" (463 upregulated and 483 downregulated DEGs), "cell part" (461 upregulated and 483 downregulated DEGs), "organelle" (283 upregulated and 307 downregulated DEGs), "membrane" (218 upregulated and 201 downregulated DEGs), and "membrane part" (134 upregulated and 136 downregulated DEGs). In the category of biological processes, they were the metabolic processes (675 upregulated and 587 downregulated DEGs), cellular processes (522 upregulated and 519 downregulated DEGs), and single-organism processes (487 upregulated and 386 downregulated DEGs). Figure 2A,B shows that differential genes are classified similarly in the two treatments. As shown in Figure 2B, there were 2134 DEGs (852 upregulated and 1282 downregulated), whereas in the DTBP treatment, there were slightly more DEGs than in the VOC treatment.

Pathway significance enrichment analysis uses pathways in the KEGG database as a unit and uses hypergeometric testing to identify pathways that are significantly enriched in DEGs compared to the entire genomic background.[34] In the VOC treatment, 412 DEGs were annotated to 105 KEGG pathways. In the DTBP treatment, 354 DEGs were annotated to 110 KEGG pathways. These particular pathways are associated with metabolism, cellular processes, and genetic information

https://doi.org/10.1021/acs.jafc.1c00640
J. Agric. Food Chem. 2021, 69, 5267−5278

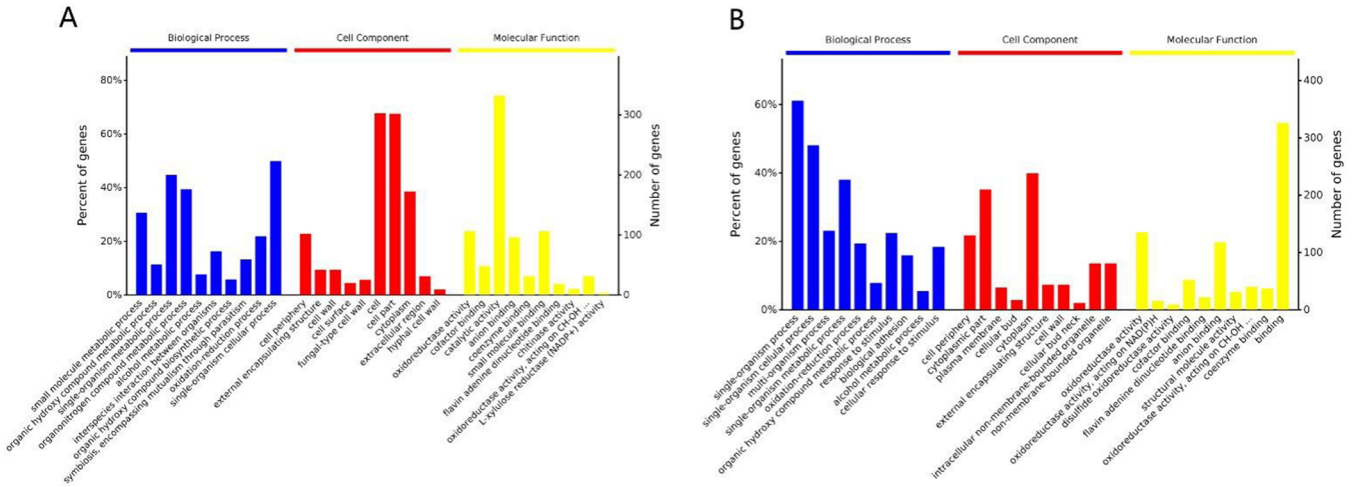

Figure 3. Functional annotation of DEPs. (A) Gene Ontology (GO) enrichment analysis for DEPs of the VOCs group. (B)GO enrichment analysis for DEPs.

processing. The scatter charts (Figure 2C,D) show the top 20 pathways with the lowest significant Q value among the significantly enriched pathways. In the VOC treatment, the most dominant pathways included glycolysis and gluconeogenesis, ribosome biogenesis in eukaryotes, fatty acid degradation, biosynthesis of unsaturated fatty acids, and nitrogen metabolism (Figure 2C). In the DTBP treatment, the most enriched pathways were involved in the biosynthesis of unsaturated fatty acids, nitrogen metabolism, fatty acid metabolism, steroid biosynthesis, ABC transporters, and glycerophospholipid metabolism.

Overview of Quantitative Proteome. Protein concentrations of the control, VOCs, and DTBP treatments are shown in Table S4. SDS-PAGE was used to assess the integrity of the extracted proteins (Figure S2). Mass spectrometry identification results are shown in Table S5. The number of Peptide-Spectrum Match was identified as 49,552; 13,692 peptides were identified as characteristic peptides, and 3963 proteins were identified, of which 3750 were quantitative proteins. Proteome Discoverer software was used to qualitatively and quantitatively calculate TMT-labeled proteomics data. The threshold for differential expression was a protein level difference > 1.2 at $P < 0.05$. As shown in Figure 1C, 565 differentially expressed proteins (DEPs) were screened in the VOC treatment (289 upregulated and 276 downregulated DEPs), and 831 DEPs were observed in the DTBP treatment (378 upregulated and 453 downregulated DEPs) compared with the control group.

Functional Annotation of DEPs. GO analysis was conducted to identify significantly enriched GO functional groups. In the VOC treatment (Figure 3A), DEPs were categorized according to biological processes, cellular components, and molecular functions. In the biological processes, the small-molecule metabolic process was the most frequent term, followed by the single-organism metabolic process and organonitrogen compound metabolic process. In the cellular component category, the most mainly enriched terms were cells, cell parts, cytoplasm, and cell periphery. Those terms about catalytic activity, oxidoreductase activity, and small-molecule binding were mainly significantly enriched. Figure 3B shows the GO statistics of significant enrichment of significant DEPs in the DTBP treatment. The terms mainly enriched in biological processes were single-organism process, single-organism cellular process, single-organism metabolic process, and response to stimulus. In the cellular component category, the most mainly enriched terms were cytoplasm, cytoplasmic part, cell periphery, and intracellular nonmembrane-bounded organelle. In molecular functions, the terms were mainly enriched regarding binding, oxidoreductase activity, and anion binding.

Figure 4A,B shows the KEEG enrichment pathway of DEPs in the VOC and DTBP treatment. 565 DEPs in the VOC treatment involved 212 pathways, which were mainly enriched regarding metabolic pathways including carbohydrate metabolism (AA), energy metabolism (AB), lipid metabolism (AC), nucleotide metabolism (AD), amino acid metabolism pathway (AE), and ribosome pathways predominantly associated with translation (BB) (Figure 4A). 831 DEPs in the DTBP treatment were associated with 258 pathways. DEPs were mainly enriched in the metabolism pathway involved in energy metabolism (AB), lipid metabolism (AC), xenobiotics biodegradation and metabolism (AK), genetic information processing pathway associated with ribosomes (BB), and protein processing in the endoplasmic reticulum (BC) (Figure 4B).

Integrated Analysis of Transcriptome and Proteome. To estimate the reproducibility of the TMT-based quantitative proteomics and RNA sequencing results, linear regression analysis based on the log2-transformed protein ratios or gene coverage depth was performed for pairwise comparison of the two experimental replicates. The observed R^2 values revealed a relatively strong linear correlation between the two experimental replicates in both quantitative proteomics and RNA sequencing. Correlation analysis was performed on DEPs and the corresponding genes in the VOC and DTBP treatments. The abscissa indicates the expression of the corresponding differential protein, and the ordinate indicates expression of the differential gene; red color indicates significantly upregulated genes and proteins in common, green means downregulation in common, and R^2 values are 0.28 and 0.51, respectively (Figure 5A,B). Proteomics provided corroborating, or at least supplementary, results regarding transcriptomics.[25] In the VOC treatment, 182 proteins were associated with the transcriptome, among which 137 showed the same trend and 45 showed the opposite trend; 309 proteins in the DTBP treatment were associated with the transcriptome. Similar

https://doi.org/10.1021/acs.jafc.1c00640
J. Agric. Food Chem. 2021, 69, 5267−5278

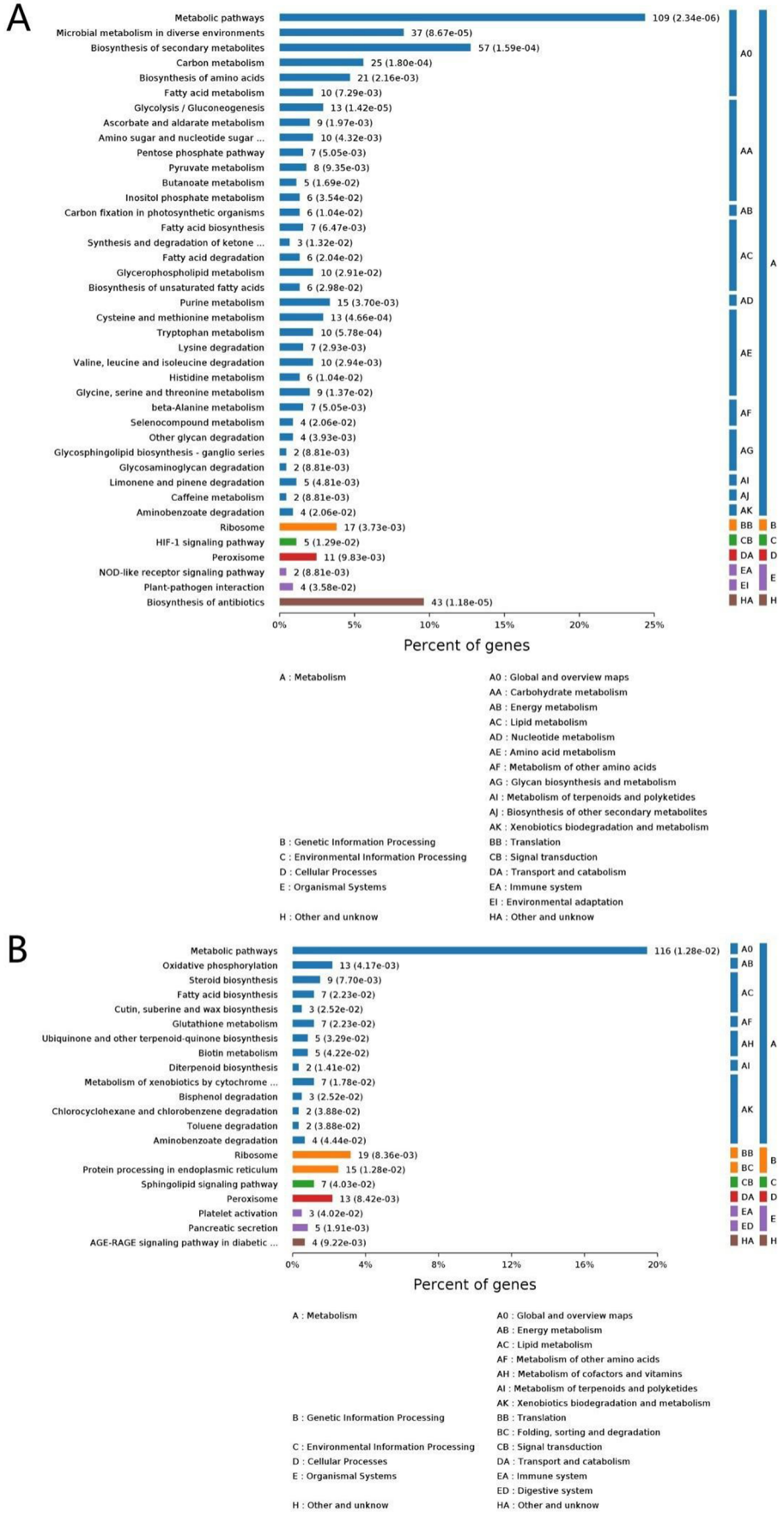

Figure 4. (A) KEGG pathway enrichment scatter plot of DEPs. (B) KEGG pathway enrichment scatter plot of DEPs in the DTBP group. Treatments are represented using different colors.

https://doi.org/10.1021/acs.jafc.1c00640
J. Agric. Food Chem. 2021, 69, 5267−5278

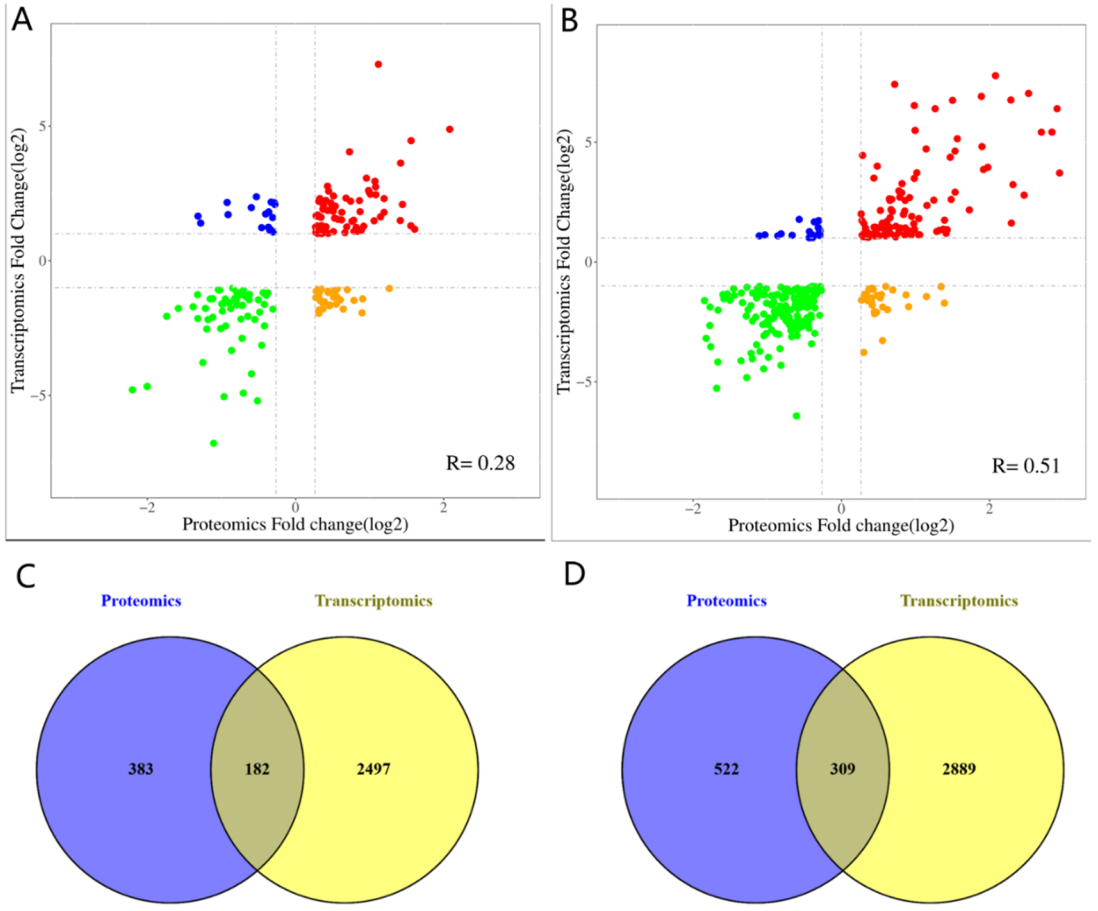

Figure 5. DEGs and DEPs correlation analysis. (A) VOCs group transcriptome and proteome shared DEGs and DEPs correlation analysis. (B) DTBP group transcriptome and proteome shared DEGs and DEPs correlation analysis. (C) Venn diagram showing unique and shared DEGs and DEPs in the VOCs group. (D) Venn diagram showing unique and shared DEGs and DEPs in the DTBP group.

trends were observed in 56 proteins, whereas opposite trends were observed in 253 proteins (Figure 5C,D). The corresponding differential genes showed relatively weak correlation patterns, but judging from the number of common genes/proteins, the number of the same trend is far more than the number of the opposite trend, so the two can be shared together analysis.

DISCUSSION

B. subtilis is a bacterium with a wide antimicrobial spectrum that can be used for eco-friendly biocontrol.[35−37] Moreover, the use of fermentation broth VOCs of *B. subtilis* has been proposed as a potential control method to counteract postharvest fruit diseases.[38] The underlying antifungal mechanism of *B. subtilis* VOCs must be elucidated in order to assess the potential for further applications. In general, biocontrol mechanisms of these microbes involve the suppression of host pathogens or boosting of immune responses through induced systemic resistance.[39] However, there were few studies that have examined the antifungal effects of VOCs produced by *B. subtilis*, and most previous studies are limited to preliminary screening and assessments of antifungal effects. In the current study, the growth of *C. gloeosporioides* was substantially inhibited by *B. subtilis* VOCs and DTBP *in vitro*. The antifungal effects of fermentation broth VOCs of *B. subtilis* CF-3 on the postharvest pathogenic fungus *C. gloeosporioides* were further analyzed using transcriptomics and proteomics.

The cell wall and the cell membrane help maintain the shape of the cell by increasing its mechanical resistance. The fungal cell wall is essential for sustaining cell morphology and protecting the cell from mechanical damage. It contains three types of major macromolecules including mannoproteins, β-glucan, and chitin.[40] Chitin is one of the major macromolecules in the cell wall.[41] We found that several pathways associated with cell wall biogenesis, such as amino sugar and nucleotide sugar metabolism as well as starch and sucrose metabolism, were considerably affected by *B. subtilis* CF-3 VOCs and DTBP. The important cell wall integrity genes encoding for chitin synthase (CGGC5_5023, CGGC5_1349, CGGC5_2120, CGGC5_4249, and CGGC5_5530) were downregulated (Table 1, spot 1−5). Also, the genes encoding glucanase (CGGC5_1733, CGGC5_ 71, CGGC5_ 10517, and CGGC5_6080) were all downregulated (Table 1, spot 6−9). In addition, some proteins (L2FJB1 and L2GAQ8) encoding chitin and glucanase were downregulated at the protein level (Table 2). In a previous study, we found that *B. subtilis* CF-3 VOC treatment could cause shrinkage and rupture in the hyphae of *C. gloeosporioides*. The structure, observed using microscopy, indicated that *B. subtilis* CF-3 VOC treatment resulted in shrunken and vacuole-forming cell organelles and deteriorated the cell wall, thereby inhibiting the

https://doi.org/10.1021/acs.jafc.1c00640
J. Agric. Food Chem. 2021, 69, 5267−5278

Table 1. Main DEGs in *C. gloeosporioides* after Treatment with *B. subtilis* CF-3 VOCs and DTBP[a]

	protein names	gene ID	log2FC VOCs/control	log2FC DTBP/control	KEGG_pathway
			Cell Wall		
1	chitin synthase	CGGC5_5023	−1.07	−1.64	amino sugar and nucleotide sugar metabolism (ko00520)
2	chitin synthase	CGGC5_1349	−1.99	−1.89	amino sugar and nucleotide sugar metabolism (ko00520)
3	chitinase 3	CGGC5_5530	−2.08	−1.13	amino sugar and nucleotide sugar metabolism (ko00520)
4	chitin synthase	CGGC5_2120	−3.41	−4.48	amino sugar and nucleotide sugar metabolism (ko00520)
5	chitin synthase	CGGC5_4249	−2.39	−1.14	amino sugar and nucleotide sugar metabolism (ko00520)
6	cellulose-growth-specific protein	CGGC5_1733	−2.87	−2.09	starch and sucrose metabolism (ko00500)
7	glucan-β-glucosidase	CGGC5_71	−1.41	−3.08	starch and sucrose metabolism (ko00500)
8	glucan-β-glucosidase	CGGC5_10517	−1.25	−1.38	starch and sucrose metabolism (ko00500)
9	endo-β-glucanase	CGGC5_6080	−1.03	−1.54	starch and sucrose metabolism (ko00500)
			Cell Membrane		
10	cytochrome P450	CGGC5_2390	−1.08	-	steroid biosynthesis (ko00100)
11	cytochrome P450	CGGC5_12188	−1.08	-	steroid biosynthesis (ko00100)
12	delta(24)-sterol reductase	CGGC5_5850	−1.17	-	steroid biosynthesis (ko00100)
13	cytochrome P450	CGGC5_3125	−1.10	-	steroid biosynthesis (ko00100); sesquiterpenoid and triterpenoid biosynthesis (ko00909)
14	tetrahydroxynaphthalene reductase	CGGC5_9	−1.42	−2.84	fatty acid biosynthesis (ko00061); biotin metabolism (ko00780); biosynthesis of unsaturated fatty acids (ko01040); fatty acid metabolism (ko01212)
15	acyloxidase	CGGC5_10911	−1.53	−1.36	fatty acid degradation (ko00071); α-linolenic acid metabolism (ko00592); biosynthesis of unsaturated fatty acids (ko01040); fatty acid metabolism (ko01212); peroxisome (ko04146)
16	delta(12) fatty acid desaturase	CGGC5_3774	−1.28	−1.48	biosynthesis of unsaturated fatty acids (ko01040); fatty acid metabolism (ko01212)
17	sterol 24-C-methyltransferase	CGGC5_12108	−1.40	−1.30	steroid biosynthesis (ko00100)
18	methylsterol monooxygenase	CGGC5_13692	−1.02	1.13	steroid biosynthesis (ko00100)
19	sterol 24-C-methyltransferase	CGGC5_1442	−2.16	−2.21	steroid biosynthesis (ko00100)
20	cytochrome P450	CGGC5_696	−1.80	−3.73	steroid biosynthesis (ko00100)
21	lanosterol 14-α-demethylase	CGGC5_8471	−1.22	−1.28	steroid biosynthesis (ko00100)
			Energy Metabolism		
22	mitochondrial chaperone bcs1	CGGC5_7365	−1.73	−2.99	-
23	cytochrome *c*	CGGC5_5334	−1.08	-	sulfur metabolism (ko00920)
24	cytochrome *c* peroxidase	CGGC5_7083	−1.06	−1.78	biosynthesis of unsaturated fatty acids (ko01040)
25	malate dehydrogenase	CGGC5_11211	−1.31	−1.30	citrate cycle (TCA cycle) (ko00020); cysteine and methionine metabolism (ko00270); pyruvate metabolism (ko00620); glyoxylate and dicarboxylate metabolism (ko00630)
26	hexokinase	CGGC5_5179	−1.99	−1.08	glycolysis/gluconeogenesis (ko00010); fructose and mannose metabolism (ko00051); galactose metabolism (ko00052)
27	hexokinase	CGGC5_6991	−1.88	−1.38	glycolysis/gluconeogenesis (ko00010); fructose and mannose metabolism (ko00051); galactose metabolism (ko00052)
28	plasma membrane H^+-ATPase pma1	CGGC5_1052	−1.67	-	oxidative phosphorylation (ko00190)
29	plasma membrane ATPase	CGGC5_2913	−1.18	−1.34	oxidative phosphorylation (ko00190)
30	nitrate reductase	CGGC5_2055	−2.29	-	nitrogen metabolism (ko00910)
31	nitrate transporter	CGGC5_5489	−1.67	−2.17	nitrogen metabolism (ko00910)
			CWDEs		
32	pectate lyase	CGGC5_1824	−1.36	-	pentose and glucuronate interconversions (ko00040)
33	pectate lyase	CGGC5_11629	−1.69	−3.11	pentose and glucuronate interconversions (ko00040)
34	pectate lyase	CGGC5_13439	−2.95	−4.90	pentose and glucuronate interconversions (ko00040)
35	cellulase (glycoside hydrolase family 5)	CGGC5_1300	−3.82	-	fructose and mannose metabolism (ko00051)

[a]"-": this gene is not DEGs in this group.

growth of *C. gloeosporioides*.[42] Therefore, the cell wall integrity of *C. gloeosporioides* was damaged after treatment with VOCs.

The lipid composition of fungal cell membranes and their content are also important factors of cell membrane integrity. Lipids have many important functions, such as increasing the stability of the cell membrane, regulating its fluidity, and reducing permeability to water-soluble substances.[42] The integrity of fungal cell membranes is closely related to the content of unsaturated fatty acids. If the cell membrane lacks unsaturated fatty acids or if the saturated fatty acid content is too high, the cell membrane may lose elasticity and membrane fluidity, and the cell ruptures subsequently.[26,43,44] The expression levels of some genes involved in cell membrane-related pathways were affected by *B. subtilis* CF-3 VOC and DTBP treatments. Those pathways mainly include fatty acid degradation, fatty acid biosynthesis, biosynthesis of unsaturated fatty acids, fatty acid metabolism, and steroid biosynthesis. Among them, the genes associated with fatty acid

https://doi.org/10.1021/acs.jafc.1c00640
J. Agric. Food Chem. 2021, 69, 5267−5278

Table 2. Main DEPs in *C. gloeosporioides* after Treatment with *B. subtilis* CF-3 VOCs and DTBP[a]

			PFC	
	uniprot ID	protein name	VOCs/con.	DTBP/con.
1	L2GAQ8	glucan-β-glucosidase	0.4611	0.4840
2	L2FJB1	chitin synthase activator	0.2978	0.8347
3	L2FPP0	FAD dependent oxidoreductase superfamily protein	0.4011	0.4973
4	L2FPI1	FAD dependent oxidoreductase superfamily protein	0.4966	0.5243
5	L2FMV1	FAD binding domain protein	0.5089	0.5657
6	L2FM08	FAD dependent oxidoreductase	0.4312	0.7194
7	L2FKP7	NADPH-dependent D-xylose	0.3979	0.8191
8	L2FD86	mitochondrial cytochrome *b*2	-	0.6550
9	L2FQQ1	mannose-6-phosphate isomerase	-	0.7277
10	L2FXK6	malic enzyme	0.7853	-

[a]"-": this protein is not DEPs in this group.

degradation [CYP51 (CGGC5_2390), WSP1 (CGGC5_12188), DWH1 (CGGC5_5850), ERG1 (CGGC5_3125), THR1 (CGGC5_9), and POX1 (CGGC5_10911)] were downregulated (Table 1, spot 10−15). FAD2 mainly encodes Δ-12 fatty acid dehydrogenase, which is related to the synthesis of linolenic acid. In addition, linolenic acid is an unsaturated fatty acid and one of the main fatty acids in *C. gloeosporioides*. It plays a vital role in maintaining cell membrane fluidity.[45] In our results, the key gene related to FAD2 (CGGC5_3774) was downregulated (Table 1, spot 16). This can affect the fluidity of the cell membrane (Figure 6). Ergosterol (ERG) is a principal sterol component of the fungal cell membrane. Generally, a decrease in the ERG content results in osmotic imbalance, disruption of cell growth, and proliferation.[46,47] *B. subtilis* CF-3 VOCs and DTBP affected the expression of ERG biosynthesis genes, thereby compromising the membrane integrity of *C. gloeosporioides*. After *B. subtilis* CF-3 VOC treatment, ERG4 (CGGC5_12108, CGGC5_13692), ERG6 (CGGC5_1442), ERG11 (CGGC5_696), and ERG25 (CGGC5_8471) were downregulated (Table 1, spot 17−21), suggesting that the integrity of the cell membrane may have been compromised. Pinto et al.[48] reported that 1,2-dihydroxy xanthone had high antibacterial activity as well as reduced the ERG contents of *Trichophyton mentagrophytes*, *Aspergillus fumigatus*, *Candida albicans*, and *Cryptococcus neoformans*. Wang et al.[20] treated *C. albicans* with MAF-1A, and the genes (ERG11, ERG1, and ERG5) involved in the ERG biosynthesis pathway were underexpressed. Our previous results suggested that *B. subtilis* CF-3 VOCs can significantly decrease cell membrane fluidity and integrity, resulting in the changes of indexes.[42] In the present results, the inhibition of ERG biosynthesis and the decrease in the unsaturated fatty acid content can lead to the decrease in membrane fluidity and function of *C. gloeosporioides*.

Energy metabolism is a basic characteristic of life. Some antifungal substances can inhibit the growth and pathogenicity of pathogenic fungi by destroying the relevant pathways of fungal energy metabolism.[49] Mitochondria are the primary sites of aerobic respiration in eukaryotic cells. They generate energy for cellular functions through oxidative phosphorylation and the tricarboxylic acid (TCA) cycle and also play a crucial role in regulating apoptosis.[50] Mitochondria are important organelles, and mitochondrial dysfunction causes cell death.[51] Several genes associated with mitochondrial functions were downregulated in *Penicillium digitatum* treated with citral.[26] In our study, several genes such as BCS1 (CGGC5_7365), CYC1 (CGGC5_5334), and CCP1 (CGGC5_7083) were downregulated (Table 1, spot 22−24). The destruction of mitochondrial structure will affect the energy metabolism of fungi, resulting in the inhibition of the growth of *C. gloeosporioides*. The pathways such as nitrogen metabolism, oxidative phosphorylation, glycolysis and gluconeogenesis, the TCA cycle, and pyruvate metabolism were significantly affected by the *B. subtilis* CF-3 VOCs and DTBP treatments. Those pathways are mainly involved in energy metabolism. *Phyllosticta citricarpa* treated with VOCs released by *Saccharomyces cerevisiae* affected the enzymes related to energy-generating pathways, particularly glycolysis and the TCA cycle.[52] In our results, expression of these key genes [MDH1 (CGGC5_11211), hxkA (CGGC5_5179, CGGC5_6991), pma-1 (CGGC5_1052, CGGC5_2913), NIA (CGGC5_2055), and crnA (CGGC5_5489)] was significantly downregulated (Table 1, spot 25−31) in the fungus after VOC and DTBP treatments. In addition, according to our results, some proteins (L2FPP0, L2FPI1, L2FMV1, L2FM08, L2FKP7, and L2FD86) were downregulated at the protein level (Table 2). Those DEPs mainly

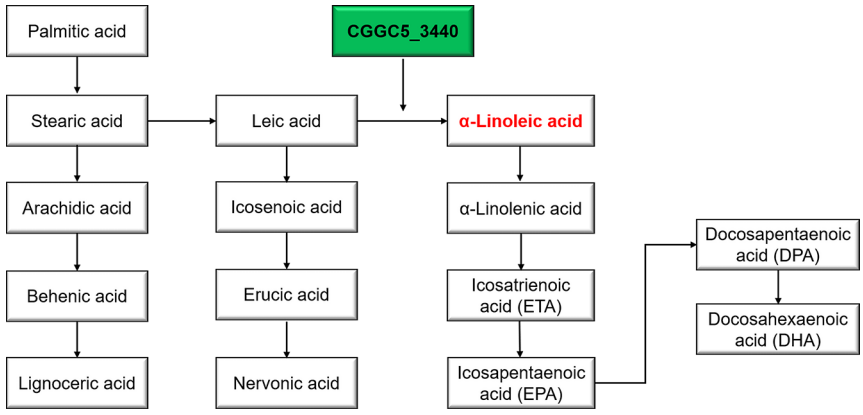

Figure 6. Pathway of biosynthesis of unsaturated fatty acids in *C. gloeosporioides*.

https://doi.org/10.1021/acs.jafc.1c00640
J. Agric. Food Chem. 2021, 69, 5267−5278

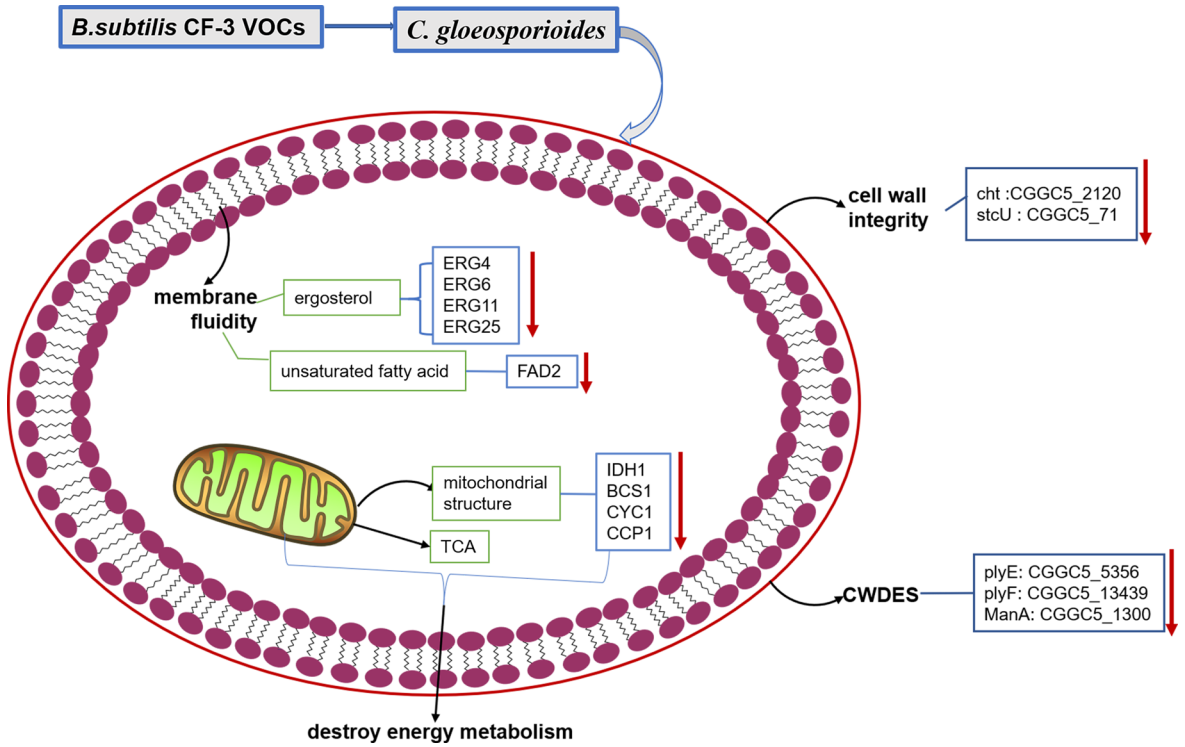

Figure 7. General overview of the effect of *B. subtilis* CF-3 VOCs treatment on *C. gloeosporioides*. The red arrows indicate downregulation of DEGs and DEPs.

concentrated in the oxidoreductase activity. They can affect the energy production of fungi. Taken together, VOC and DTBP treatments significantly inhibited energy production processes in fungal cells.

In the process of mutual recognition of plant hosts and pathogens, pathogenic fungi can secrete cell wall-degrading enzymes (CWDEs), mainly including cellulase, pectinase, cutinase, and so on. Cellulase, pectinase, and cutinase play an important role in anthracnose.[53,54] Therefore, CWDEs are important components of plant pathogenic fungi.[55,56] Pectate lyase (PL) is common in plant pathogenic bacteria, fungi, and nematodes;[57] moreover, it is an important pathogenic factor that degrades the host cell wall and increases the susceptibility of plants to pathogens.[58] The important genes associated with PL coding, plyD (CGGC5_1824), plyE (CGGC5_11629), and plyF (CGGC5_13439) were found to be downregulated in both analyses (Table 1, spot 32−34). Many DEGs associated with multiple CWDEs were downregulated in the VOC and DTBP treatments. Furthermore, cellulase-related gene [manA (CGGC5_1300)] was also downregulated (Table 1, spot 35). Downregulation of these genes can inhibit *C. gloeosporioides*, which corresponds to weakening of the ability of *C. gloeosporioides* to infect the host. The result indicates that VOCs can reduce *C. gloeosporioides* virulence by inhibiting the secretion of some extracellular enzymes.

In conclusion, transcriptomic and proteomic analysis were complementary approaches to investigate inhibition effects of *B. subtilis* CF-3 VOCs on the postharvest pathogenic fungus *C. gloeosporioides* (Figure 7). The results showed that *B. subtilis* CF-3 VOCs inhibited important fungal pathways, mainly including effects on cell membranes, cell wall synthesis and energy metabolism. In addition, downregulation of genes encoding CWDEs may substantially weaken the ability of *C. gloeosporioides* to infect the host. We concluded that the disruption of the growth and development by *B. subtilis* CF-3 VOCs contributes to its antifungal activity against *C. gloeosporioides*. Our results provide important insights for revealing the mechanisms underlying the inhibitory effects of *B. subtilis* CF-3 VOCs on fungal growth, which may be of use for future applications.

■ ASSOCIATED CONTENT

Supporting Information

The Supporting Information is available free of charge at https://pubs.acs.org/doi/10.1021/acs.jafc.1c00640.

Additional experimental results (PDF)

■ AUTHOR INFORMATION

Corresponding Author

Haiyan Gao − *School of Life Sciences, Shanghai University, Shanghai 200444, China;* orcid.org/0000-0002-1114-3387; Email: hygao1111@126.com

Authors

Ke Wang − *School of Life Sciences, Shanghai University, Shanghai 200444, China*

Zhen Qin − *School of Life Sciences, Shanghai University, Shanghai 200444, China;* orcid.org/0000-0003-2133-8572

Shiyuan Wu − *School of Life Sciences, Shanghai University, Shanghai 200444, China*

Pengyu Zhao − *School of Life Sciences, Shanghai University, Shanghai 200444, China*

Chaoying Zhen − *School of Life Sciences, Shanghai University, Shanghai 200444, China*

Complete contact information is available at: https://pubs.acs.org/10.1021/acs.jafc.1c00640

Author Contributions

[†]K.W. and Z.Q. contributed equally in this study.

Funding

This study was supported by the National Natural Science Foundation of China (project no.31972120), the project of Science and Technology Innovation Action Plan of Shanghai Science and Technology Commission of China (no. 18391901300).

Notes

The authors declare no competing financial interest.

■ ACKNOWLEDGMENTS

We thank Jianwen Hu at Shanghai Bioprofile Technology Company Ltd. for his technical support in mass spectroscopy.

■ ABBREVIATIONS

VOCs, volatile organic compounds; DTBP, 2,4-di-*tert*-butylphenol; DEGs, differentially expressed genes; DEPs, differentially expressed proteins; PDA, potato dextrose agar medium; LB, Luria-Bertani; GO, gene ontology; CWDEs, cell wall degrading enzymes; PL, pectate lyase; ERG, ergosterol; TCA, tricarboxylic acid

■ REFERENCES

(1) Liu, S.; Shao, X.; Wei, Y.; Li, Y.; Xu, F.; Wang, H. Solidago canadensis L. Essential oil vapor effectively inhibits Botrytis cinerea growth and preserves postharvest quality of strawberry as a food model system. *Front. Microbiol.* **2016**, *7*, 1179−1187.

(2) Tournas, V. H.; Katsoudas, E. Mould and yeast flora in fresh berries, grapes and citrus fruits. *Int. J. Food Microbiol.* **2005**, *105*, 11−17.

(3) Yan, J.; Yuan, S.; Wang, C.; Ding, X.; Cao, J.; Jiang, W. Enhanced resistance of jujube (Zizyphus jujuba Mill. cv. Dongzao) fruit against postharvest Alternaria rot by β-aminobutyric acid dipping. *Sci. Hortic.* **2015**, *186*, 108−114.

(4) De Miccolis Angelini, R. M.; Domenico, A.; Caterina, R.; Donato, G.; Stefania, P.; Francesco, F. De novo assembly and comparative transcriptome analysis of Monilinia fructicola, Monilinia laxa and Monilinia fructigena, the causal agents of brown rot on stone fruits. *BMC Genomics* **2018**, *19*, 436−456.

(5) Lopes, L. H. R.; Boiteux, L. S.; Rossato, M.; Aguiar, F. M.; Fonseca, M. E. N.; Oliveira, V. R.; Reis, A. Diversity of Colletotrichum species causing onion anthracnose in Brazil. *Eur. J. Plant Pathol.* **2021**, *159*, 339−357.

(6) Li, X.; Jing, T.; Zhou, D.; Zhang, M.; Qi, D.; Zang, X.; Zhao, Y.; Li, K.; Tang, W.; Chen, Y.; Qi, C.; Wang, W.; Xie, J. Biocontrol efficacy and possible mechanism of Streptomyces sp. H4 against postharvest anthracnose caused by Colletotrichum fragariae on strawberry fruit. *Postharvest. Biol. Technol.* **2021**, *175*, 111401.

(7) Ali, A.; Bordoh, P. K.; Singh, A.; Siddiqui, Y.; Droby, S. Postharvest development of anthracnose in pepper (Capsicum spp): Etiology and management strategies. *Crop Prot.* **2016**, *90*, 132−141.

(8) Qi, N. L.; Li, T.; Zhou, H. L.; Yang, C. L. Survey of sulfur dioxide residues in litchi preservation process in Hainan province. *Appl. Mech. Mater.* **2015**, *713*−*715*, 2920−2923.

(9) Siddiqui, Y.; Ali, A. Colletotrichum Gloeosporioides (Anthracnose). *Postharvest Decay*; Academic Press, 2014; pp 337−371.

(10) Ma, X.; Wang, X.; Cheng, J.; Nie, X.; Yu, X.; Zhao, Y.; Wang, W. Microencapsulation of Bacillus subtilis B99-2 and its biocontrol efficiency against Rhizoctonia solani in tomato. *Biol. Control* **2015**, *90*, 34−41.

(11) Zhou, X.; Lu, Z.; Lv, F.; Zhao, H.; Wang, Y.; Bie, X. Antagonistic action of Bacillus subtilis strain fmbj on the postharvest pathogen Rhizopus stolonifer. *J. Food Sci.* **2011**, *76*, M254−M259.

(12) Zhang, B.; Li, Y.; Zhang, Y.; Qiao, H.; He, J.; Yuan, Q.; Chen, X.; Fan, J. High-cell-density culture enhances the antimicrobial and freshness effects of Bacillus subtilis S1702 on table grapes (Vitis vinifera cv. Kyoho). *Food Chem.* **2019**, *286*, 541−549.

(13) Li, X.-Y.; Mao, Z.-C.; Wu, Y.-X.; Ho, H.-H.; He, Y.-Q. Comprehensive volatile organic compounds profiling of Bacillus species with biocontrol properties by head space solid phase microextraction with gas chromatography-mass spectrometry. *Biocontrol Sci. Technol.* **2015**, *25*, 132−143.

(14) Gao, H.; Xu, X.; Dai, Y.; He, H. Isolation, Identification and characterization of Bacillus subtilis CF-3, a bacterium from fermented bean curd for controlling postharvest diseases of peach fruit. *Food Sci. Technol. Res.* **2016**, *22*, 377−385.

(15) Gao, H.; Xu, X.; Zeng, Q.; Li, P. Optimization of headspace solid-phase microextraction for GC-MS analysis of volatile compounds produced by biocontrol strain Bacillus subtilis CF-3 using response surface methodology. *Food Sci. Technol. Res.* **2017**, *23*, 583−593.

(16) Xu, X.; Zeng, X.; Li, P.; Zeng, Q.; Yin, J.; Gao, H. Purification and identification of fungistatic protein from Bacillus subtilis CF-3. *Mod. Food Sci. Technol.* **2016**, *12*, 145−150.

(17) Gao, P.; Li, X.; Xu, Q.; Zeng, W.; Guan, H. Research on volatile organic compounds from Bacillus subtilis CF-3: biocontrol effects on fruit fungal pathogens and dynamic changes during fermentation. *Front. Microbiol.* **2018**, *9*, 456−470.

(18) Parafati, L.; Vitale, A.; Restuccia, C.; Cirvilleri, G. Performance evaluation of volatile organic compounds by antagonistic yeasts immobilized on hydrogel spheres against gray, green and blue postharvest decays. *Food Microbiol.* **2017**, *63*, 191−198.

(19) Wang, Z.; Gerstein, M.; Snyder, M. RNA-Seq: a revolutionary tool for transcriptomics. *Nat. Rev. Genet.* **2009**, *10*, 57−63.

(20) Wang, T.; Xiu, J.; Zhang, Y.; Wu, J.; Ma, X.; Wang, Y.; Guo, G.; Shang, X. Transcriptional responses of Candida albicans to antimicrobial peptide MAF-1A. *Front. Microbiol.* **2017**, *8*, 894.

(21) Guerreiro, A. C. L.; Benevento, M.; Lehmann, R.; van Breukelen, B.; Post, H.; Giansanti, P.; Maarten Altelaar, A. F.; Axmann, I. M.; Heck, A. J. R. Daily rhythms in the cyanobacterium Synechococcus elongatus probed by high-resolution mass spectrometry-based proteomics reveals a small defined set of cyclic proteins. *Mol. Cell. Proteomics* **2014**, *13*, 2042−2055.

(22) Nie, S.; Lo, A.; Wu, J.; Zhu, J.; Tan, Z.; Simeone, D. M.; Anderson, M. A.; Shedden, K. A.; Ruffin, M. T.; Lubman, D. M. Glycoprotein biomarker panel for pancreatic cancer discovered by quantitative proteomics analysis. *J. Proteome Res.* **2014**, *13*, 1873−1884.

(23) Dai, W.; Chen, Q.; Wang, Q.; White, R. R.; Liu, J.; Liu, H. Complementary transcriptomic and proteomic analyses reveal regulatory mechanisms of milk protein production in dairy cows consuming different forages. *Sci. Rep.* **2017**, *7*, 44234.

(24) Zhang, M.; Ge, J.; Yu, X. Transcriptome analysis reveals the mechanism of fungicidal of thymol against Fusarium oxysporum f. sp. niveum. *Curr. Microbiol.* **2018**, *75*, 410−419.

(25) Zhao, X.; Li, C.; Yan, C.; Wang, J.; Yuan, C.; Zhang, H.; Shan, S. Transcriptome and proteome analyses of resistant preharvest peanut seed coat in response to Aspergillus flavus infection. *Electron. J. Biotechnol.* **2019**, *39*, 82−90.

(26) OuYang, Q.; Tao, N.; Jing, G. Transcriptional profiling analysis of Penicillium digitatum, the causal agent of citrus green mold, unravels an inhibited ergosterol biosynthesis pathway in response to citral. *BMC Genomics* **2016**, *17*, 599.

(27) Arrebola, E.; Sivakumar, D.; Korsten, L. Effect of volatile compounds produced by Bacillus strains on postharvest decay in citrus. *Biol. Control* **2010**, *53*, 122−128.

(28) Jiang, C.; Shi, J.; Liu, Y.; Zhu, C. Inhibition of Aspergillus carbonarius and fungal contamination in table grapes using Bacillus subtilis. *Food Control* **2014**, *35*, 41−48.

(29) Florea, L.; Song, L.; Salzberg, S. L. Thousands of exon skipping events differentiate among splicing patterns in sixteen human tissues. *F1000Research* **2013**, *2*, 188.

(30) Leng, N.; Dawson, J. A.; Thomson, J. A.; Ruotti, V.; Rissman, A. I.; Smits, B. M. G.; Haag, J. D.; Gould, M. N.; Stewart, R. M.;

https://doi.org/10.1021/acs.jafc.1c00640
J. Agric. Food Chem. 2021, 69, 5267−5278

Kendziorski, C. EBSeq: an empirical Bayes hierarchical model for inference in RNA-seq experiments. *Bioinformatics* **2013**, *29*, 1035−1043.
(31) Mao, X.; Cai, T.; Olyarchuk, J. G.; Wei, L. Automated genome annotation and pathway identification using the KEGG Orthology (KO) as a controlled vocabulary. *Bioinformatics* **2005**, *21*, 3787−3793.
(32) Sherlock, G. Gene Ontology: tool for the unification of biology. *Food Res. Int.* **2009**, *22*, 415.
(33) Kanehisa, M.; Goto, S.; Sato, Y.; Furumichi, M.; Tanabe, M. KEGG for integration and interpretation of large-scale molecular data sets. *Nucleic Acids Res.* **2012**, *40*, D109−D114.
(34) Kanehisa, M.; Araki, M.; Goto, S.; Hattori, M.; Hirakawa, M.; Itoh, M.; Katayama, T.; Kawashima, S.; Okuda, S.; Tokimatsu, T.; Yamanishi, Y. KEGG for linking genomes to life and the environment. *Nucleic Acids Res.* **2008**, *36*, D480−D484.
(35) Chen, H.; Xiao, X.; Wang, J.; Wu, L.; Zheng, Z.; Yu, Z. Antagonistic effects of volatiles generated by Bacillus subtilis on spore germination and hyphal growth of the plant pathogen, Botrytis cinerea. *Biotechnol. Lett.* **2008**, *30*, 919−923.
(36) Senthil, R.; Prabakar, K.; Rajendran, L.; Karthikeyan, G. Efficacy of different biological control agents against major postharvest pathogens of grapes under room temperature storage conditions. *Phytopathol. Mediterr.* **2011**, *50*, 55−65.
(37) Maachia, B.; Rafik, E.; Chérif, M.; Nandal, P.; Mohapatra, T.; Bernard, P. Biological control of the grapevine diseases "grey mold" and "powdery mildew" by Bacillus B27 and B29 strains. *Indian J. Exp. Biol.* **2015**, *53*, 109−115.
(38) Zheng, M.; Shi, J.; Shi, J.; Wang, Q.; Li, Y. Antimicrobial effects of volatiles produced by two antagonistic Bacillus strains on the anthracnose pathogen in postharvest mangos. *Biol. Control* **2013**, *65*, 200−206.
(39) Salwan, R.; Sharma, V. Genome wide underpinning of antagonistic and plant beneficial attributes of Bacillus sp. SBA12. *Genomics* **2020**, *112*, 2894−2902.
(40) Klis, F. M.; de Groot, P.; Hellingwerf, K. Molecular organization of the cell wall of Candida albicans. *Med. Mycol.* **2001**, *39*, 1−8.
(41) Rizzi, Y. S.; Happel, P.; Lenz, S.; Urs, M. J.; Bonin, M.; Cord-Landwehr, S.; Singh, R.; Moerschbacher, B. M.; Kahmann, R. Chitosan and Chitin Deacetylase Activity Are Necessary for Development and Virulence of Ustilago maydis. *Mbio* **2021**, *12*, No. e03419.
(42) Zhao, P.; Li, P.; Wu, S.; Zhou, M.; Zhi, R.; Gao, H. Volatile organic compounds (VOCs) from Bacillus subtilis CF-3 reduce anthracnose and elicit active defense responses in harvested litchi fruits. *AMB Express* **2019**, *9*, 119.
(43) Cronan, J. E. Bacterial membrane lipids: where do we stand? *Annu. Rev. Microbiol.* **2015**, *57*, 203−224.
(44) Bayer, A. S.; Prasad, R.; Chandra, J.; Koul, A.; Smriti, M.; Varma, A.; Skurray, R. A.; Firth, N.; Brown, M. H.; Koo, S.-P.; Yeaman, M. R. In vitro resistance of Staphylococcus aureus to thrombin-induced platelet microbicidal protein is associated with alterations in cytoplasmic membrane fluidity. *Infect. Immun.* **2000**, *68*, 3548−3553.
(45) Xue, Y.; Zhang, X.; Wang, R.; Chen, B.; Jiang, J.; Win, A. N.; Chai, Y. Cloning and expression of Perilla frutescens FAD2 gene and polymorphism analysis among cultivars. *Acta Physiol. Plant.* **2017**, *39*, 84−102.
(46) Sun, X.; Wang, J.; Feng, D.; Ma, Z.; Li, H. PdCYP51B, a new putative sterol 14α-demethylase gene of Penicillium digitatum involved in resistance to imazalil and other fungicides inhibiting ergosterol synthesis. *Appl. Microbiol. Biotechnol.* **2011**, *91*, 1107−1119.
(47) Tao, N.; OuYang, Q.; Jia, L. Citral inhibits mycelial growth of Penicillium italicum by a membrane damage mechanism. *Food Control* **2014**, *41*, 116−121.
(48) Pinto, E.; Afonso, C.; Duarte, S.; Vale-Silva, L.; Costa, E.; Sousa, E.; Pinto, M. Antifungal activity of xanthones: evaluation of their effect on ergosterol biosynthesis by high-performance liquid chromatography. *Chem. Biol. Drug Des.* **2011**, *77*, 212−222.
(49) Xu, J.; Shao, X.; Wei, Y.; Xu, F.; Wang, H. iTRAQ proteomic analysis reveals that metabolic pathways involving energy metabolism are affected by tea tree oil in Botrytis cinerea. *Front. Microbiol.* **2017**, *8*, 1989.
(50) Shaughnessy, D. T.; McAllister, K.; Worth, L.; Haugen, A. C.; Meyer, J. N.; Domann, F. E.; Van Houten, B.; Mostoslavsky, R.; Bultman, S. J.; Baccarelli, A. A.; Begley, T. J.; Sobol, R. W.; Hirschey, M. D.; Ideker, T.; Santos, J. H.; Copeland, W. C.; Tice, R. R.; Balshaw, D. M.; Tyson, F. L. Mitochondria, energetics, epigenetics, and cellular responses to stress. *Environ. Health Perspect.* **2014**, *122*, 1271−1278.
(51) Wu, X.-Z.; Cheng, A.-X.; Sun, L.-M.; Sun, S.-J.; Lou, H.-X. Plagiochin E, an antifungal bis(bibenzyl), exerts its antifungal activity through mitochondrial dysfunction-induced reactive oxygen species accumulation in Candida albicans. *Biochim. Biophys. Acta* **2009**, *1790*, 770−777.
(52) Fialho, M. B.; de Andrade, A.; Bonatto, J. M. C.; Salvato, F.; Labate, C. A.; Pascholati, S. F. Proteomic response of the phytopathogen Phyllosticta citricarpa to antimicrobial volatile organic compounds from Saccharomyces cerevisiae. *Microbiol. Res.* **2016**, *183*, 1−7.
(53) Curro, G.; Cannistra, S. Study of the hygienic conditions of the nursery schools of the city of Reggio Calabria. *Ig. Mod.* **1966**, *59*, 563−572.
(54) Hamann, T. Plant cell wall integrity maintenance as an essential component of biotic stress response mechanisms. *Front. Plant Sci.* **2012**, *3*, 77.
(55) Yang, Y.-Q.; Yang, M.; Li, M.-H.; Zhou, E.-X. Cloning and functional analysis of an endo-PG-encoding gene Rrspg1 of Rhizoctonia solani, the causal agent of rice sheath blight. *Can. J. Plant Pathol.* **2012**, *34*, 436−447.
(56) Hématy, K.; Cherk, C.; Somerville, S. Host-pathogen warfare at the plant cell wall. *Curr. Opin. Plant Biol.* **2009**, *12*, 406−413.
(57) Saoudi, B.; Habbeche, A.; Kerouaz, B.; Haberra, S.; Ben Romdhane, Z.; Tichati, L.; Boudelaa, M.; Belghith, H.; Gargouri, A.; Ladjama, A. Purification and characterization of a new thermoalkaliphilic pectate lyase from Actinomadura keratinilytica Cpt20. *Process Biochem.* **2015**, *50*, 2259−2266.
(58) Kikot, G. E.; Hours, R. A.; Alconada, T. M. Contribution of cell wall degrading enzymes to pathogenesis of Fusarium graminearum: a review. *J. Basic Microbiol.* **2009**, *49*, 231−241.

https://doi.org/10.1021/acs.jafc.1c00640
J. Agric. Food Chem. 2021, 69, 5267−5278